Multipole analysis of $^2H(\gamma,p)n$ in the Δ resonance region

C. S. Whisnant, W. K. Mize, and D. Pomaréde*
Department of Physics and Astronomy, University of South Carolina, Columbia, South Carolina 29208

A. M. Sandorfi
Department of Physics, Brookhaven National Laboratory, Upton, New York 11973

(Received 8 December 1997)

An energy-dependent multipole analysis of the photodisintegration of deuterium has been performed for photon energies between 187 and 314 MeV using recent data taken with linearly polarized photons. A good fit is obtained with 11 free parameters determining eight multipoles. A wide variety of multipole solutions has been examined and in all cases the cross section with photon polarization parallel to the reaction plane is dominated by electric transitions, with $E2 \cdot E1$ interference responsible for the observed forward-backward angular asymmetry. The cross sections observed in perpendicular kinematics are dominated by magnetic multipoles. Several recent $N\Delta/NN$ coupled-channel calculations have predicted a pronounced 90° dip in the cross section that is absent from the data. This dip can be reproduced by changing the $M2$ strength distribution in our fit. A comparison is made with multipoles calculated by Wilhelm and Arenhövel at 300 MeV. [S0556-2813(98)00507-X]

PACS number(s): 25.20.−x, 21.30.Cb, 24.10.Eq, 25.10.+s

Deuteron photodisintegration has been one of the traditional testing grounds for studies of the NN and $N\Delta$ interactions. Near typical Δ excitation energies ($E_\gamma \sim 300$ MeV), two factors contribute to making this an important laboratory for the study of both forces. First, since the incident photon interacts primarily with one of the two nucleons, at these energies it is the magnetic dipole $\gamma N\Delta$ coupling that dominates and leads directly to an $N\Delta$ intermediate state. The second factor comes from the spin structure of the deuteron, which is primarily $^3S_1$ with a small additional $^3D_1$ component generated by the NN tensor force. Since the $M1$ operator primarily flips spin without changing orbital angular momentum, $M1(^3S_1) \rightarrow {}^1S_0$ transitions cannot pass through an $N\Delta$ intermediate state and $\Delta l = 2$ $M1(^3S_1) \rightarrow {}^1D_2$ transitions are strongly suppressed. Thus, $M1$ Δ excitation proceeds mainly through the D state of the deuteron wave function via a $\Delta l = 0$ $M1(^3D_1) \rightarrow {}^1D_2$ transition and is inherently sensitive to the NN tensor interaction.

Leidemann and Arenhövel [1], and Peña *et al.* [2], have confirmed the expected sensitivity to the $N\Delta$ interaction in $D(\gamma,p)n$, both in the cross section and in the beam polarization asymmetry. Calculations similar to Ref. [1], combined with the first simultaneous measurements of both observables by the LEGS Collaboration [3], have also demonstrated a strong sensitivity to the short-range part of the NN tensor force, an aspect of the interaction that is not well constrained by other experiments.

A full microscopic model for $D(\gamma,p)n$ requires a unitary coupled-channel treatment of the NN and $N\Delta$ interactions, and several sophisticated calculations have been developed in recent years [2,4–6]. These calculations have several features in common, but they also exhibit significant differences as well, notably in the distribution of partial wave strength. Characteristic of these calculations is a discrepancy in the cross section that grows with energy above about 250 MeV creating a dip in the predicted 90° cross section that is absent from the data. A detailed comparison of the calculations of Wilhelm and Arenhövel [4] (WA) with the LEGS data at 300 MeV shows that while the predicted cross section with photon polarization parallel to the reaction plane $\sigma_\parallel$ is in reasonable agreement with the data, the cross section in perpendicular polarization kinematics $\sigma_\perp$ is predicted to be too high at forward and backward angles and too low at 90° [7]. Although in the γN system, Δ excitation is almost purely $M1$, when transformed to the deuteron center of mass many magnetic as well as electric multipoles can contribute, and their interference with the dominant $M1(^3D_1) \rightarrow {}^1D_2$ transition will strongly effect predictions, particularly for polarization observables. This makes it impossible to understand the source of such discrepancies through a direct comparison with the data alone.

It has long been recognized [8,9] that an experimental multipole decomposition of this reaction would be an extremely useful tool in analyzing the successes and shortcomings of theoretical calculations. Previous authors have characterized the data with energy-dependent Legendre polynomial fits (see Ref. [10], and references therein). Such fits are useful in providing an average of data from many different experiments for displaying general properties of the data but provide very little insight. The results of a Legendre polynomial fit are helpful only when interpreted in the context of a model. A purely data-driven analysis cannot indicate a possible source of agreement or disagreement with a calculation. Our goal in the present work is to extract information from the data in the form of a multipole expansion for a detailed comparison with theory. This has not previously been attempted, mainly because of the ambiguities that result from combining measurements of observables from different experiments that have different systematic uncer-

*Present address: Centre de Physique, Ecole Polytechnique, F-91128 Palaiseau-Cedex, France.

tainties. This situation has been changed by the recent availability of a precision data set from LEGS which reports both cross sections and beam asymmetries covering the energy region of the Δ resonance [7,11].

We present here the first multipole decomposition of the $D(\gamma,p)n$ reaction. This analysis is necessarily model dependent due to the limited number of observables available. There are 24 complex amplitudes $(2_\gamma \times 2_p \times 2_n \times 3_d)$ which reduce to 12 under parity and time reversal invariance. Thus, there are 24 real parameters to determine. For a unique solution (to within an overall phase), 23 experiments are required. With only two observables, the problem is severely underdetermined. Nevertheless, it is possible to produce a physically meaningful, model-dependent fit.

We have included electric and magnetic dipole and quadrupole photons in the initial state and all possible relative p-n angular momenta in the final state. This produces a multipole expansion containing 22 complex amplitudes, which are normalized [12] so that

$$\sigma_{\rm tot} = \sigma_{M1} + \sigma_{E1} + \sigma_{M2} + \sigma_{E2}, \tag{1a}$$

where

$$\sigma_{ML,EL} = \frac{\pi}{6}\left(\frac{\hbar c}{E_\gamma}\right)^2 \sum (2J+1)|ML,EL(^{2S+1}\ell_J)|^2. \tag{1b}$$

Here, L is the total photon angular momentum, ℓ is the p-n relative orbital angular momentum, and J is the total final state spin. Since the data lie mainly below the 2π threshold where the inelasticities in most partial waves are small, we use Watson's theorem [13] to specify the phases. These are taken from the p-n scattering phases of the VPI FA95 solution [14]. This leaves 22 magnitudes to be determined from the data. Preliminary energy-independent analyses revealed that these magnitudes are strongly correlated through their similar angular dependences and, if left unconstrained, can oscillate wildly from energy to energy. To ensure that the fitted multipoles vary smoothly with energy, an explicit energy dependence must be assumed. While a Breit-Wigner form might be a tempting parametrization for the $M1(^1D_2)$ where the Δ is dominant, there are in fact several reasons to expect significant deviations from such a pure resonance shape. First, there are nonresonant contributions even to the $M1$ in the γN system, and these will persist in the γD system. Secondly, the mixing of the multipoles in the transformation from the γN to γD systems could further dilute the resonance portion of the $M1$, spreading it among many other multipoles. Finally, even if one were to impose a resonant shape on certain multipoles, there is still the problem of the choice and interpretation of the Δ width(s) which is itself energy dependent [8]. With these caveats and the desire to keep the parametrization as simple as possible, the energy dependence for each multipole m has been parametrized as

$$ML,EL(^{2S+1}\ell_J) = c_m + l_m x + q_m x^2, \tag{2}$$

where x is the scaled, dimensionless variable, $x=(E_\gamma - E_{\rm min})/(E_{\rm max}-E_{\rm min})$. $E_{\rm max}$ and $E_{\rm min}$ are the maximum and minimum energies included in the fit, respectively. The coefficients of the terms constant, linear, and quadratic in energy are represented by c, l, and q, respectively. The extent to which the Δ resonance strength is redistributed among the γD multipoles is an interesting question which we would like the data to answer. This form is the simplest choice that allows a peak in each multipole.

The parametrization in Eq. (2) results in 66 constants. To limit this enormous number of parameters, we are guided by three observations. First, the $M1$ multipoles are expected to dominate, in particular the $M1(^1D_2)$. Secondly, a semiclassical estimate shows that a 300 MeV photon absorbed at the edge of the deuteron has an angular momentum of approximately 2.5, so that contributions from final states with significantly higher relative p-n angular momenta are expected to be very small [the expansion in Eq. (1) contains terms up to $\ell=4$]. Finally, the general energy dependence of the WA multipoles was used to infer the initial energy dependence in Eq. (2), beyond the overall $1/E_\gamma$ dependence of Eq. (1). With such guidance, a physically meaningful solution with many fewer than 66 parameters is obtained.

The fit was made to the complete LEGS data set [11] consisting of cross section sum, $d\sigma/d\Omega = (1/2)(d\sigma_\parallel/d\Omega + d\sigma_\perp/d\Omega)$, and difference $\Delta = (1/2)(d\sigma_\parallel/d\Omega - d\sigma_\perp/d\Omega)$ angular distributions at 13 energies and integrated total cross sections at 12 energies between 187.5 and 313.8 MeV. There are data at eight angles for all but the lowest two energies where there are seven. This gives a total of 216 data points in the fit. A χ^2 minimization was made to these data using the CERN program MINUIT [15].

For better control of the fitting process, the initial fit was done in three steps. We began with the $M1(^1D_2)$ and some of the higher angular momentum terms in the $E1$, $M2$, and $E2$ multipoles. In the second and third steps, terms, expected to be smaller according to the general criteria outlined above, were added. At each step, all parameters were allowed to vary. After investigating the model space to get an idea of the relative importance of the various terms, a procedure was found which produced a fit with 21 parameters. This is outlined in the column labeled initial in Table I. This fit contained four parameters for which the uncertainty exceeded the value of the parameter. Fixing these undetermined parameters to zero and refitting gave the 17 parameter fit described in the column labeled pruned.

This procedure still left poorly determined parameters in the fit, some with uncertainties in excess of 50%. To reduce the parameter set to a minimum and improve the uncertainties, we have used the F test [16] to estimate the significance of each term. The order in which parameters are removed from the fit is determined in the following way. Starting from the pruned fit, a parameter is temporarily fixed to zero and the fit is repeated with one fewer degree of freedom. This is done successively for all the terms in the fit. The term which has the least effect on χ^2 is permanently removed from the fit. The significance of the deleted term is evaluated by computing the F statistic. By successively removing the terms which change χ^2 the least, parameters were removed until F showed a significant increase beyond the critical value corresponding to 99% probability that the additional term was required. In this way, the number of parameters was reduced to 11. The energy dependences of the remaining parameters and their uncertainties are given in the column labeled final

TABLE I. Outline of the fitting procedure. The energy dependence is indicated by the letters c,l,q, representing the inclusion of the constant, linear, and quadratic terms, respectively. The reduced χ^2 for each step in the initial fit is given along with the final value. The numbers in parentheses in the final column are the percent uncertainties for each parameter.

	Energy dependence		
Multipole	Initial	Pruned	Final
$M1(^1D_2)$	c,l,q	c,l,q	$c(4.5),l(3.3),q(4,6)$
$E1(^3F_2)$	c,l	c	$c(1.8)$
$M2(^3F_3)$	c,l	c,l	$c(8.4),l(3.4)$
$E2(^3D_1)$	c,l	l	$l(11.5)$
$E2(^3D_3)$	c,l	c	$c(5.8)$
$E2(^3G_3)$	c,l	c,l	$c(3.1)$
χ^2/n_f	2.57		
$E2(^1D_2)$	c,l,q	c,l,q	
$E1(^3P_0)$	c,l	c,l	$c(3.8)$
χ^2/n_f	2.31		
$E1(^3P_1)$	c,l,q	l,q	$l(6.8)$
χ^2/n_f	2.06	2.04	2.39

in Table I. All of these parameters are determined to better than 12% and all but three have uncertainties between 3 and 7 % as indicated in the table.

As a final step, fits were made successively freeing each of the previously unused multipoles along with all parameters in the final set to search for any overlooked dependences. Although the inclusion of additional parameters improved the χ^2, the F test indicated that none of the improvements were statistically significant.

It should be noted that by ignoring the known deuteron spin structure and successively adding multipoles which reduce χ^2 the most, removing the undetermined parameters and then using the F test to find the minimum set, a nine parameter fit to the data can be made. This purely data driven fit shows a very strong preference for the $M1(^3D_2)$ over the $M1(^1D_2)$. This occurs because the $M1(^3D_2)$ produces a flatter $\sigma_\perp$ than the $M1(^1D_2)$, giving an angular distribution more like the data. However, we have rejected this solution as unphysical.

A measure of the overall quality of the fit is seen by examining the difference between the data and the fit for the 204 sum and difference cross section data points. The standard deviation for this distribution is 0.20 μb/sr which is quite comparable to the average statistical experimental uncertainty of 0.13 μb/sr. Using the complete covariance matrix to compute the uncertainties on the fit, the angle integrated total cross sections are determined to about $\pm 0.3\%$. These uncertainties on the fit reflect only the statistical and polarization-dependent uncertainties on the data. We have also made fits adding a variable scale factor for the data, weighting its contribution to χ^2 by the 5% experimental systematic uncertainty following the method described by D'Agostini [17]. This produces a scale factor of one to well within the experimental limit, a uniform 5% uncertainty on the fit results, and the same values for the parameters in the fit as found when including only the statistical uncertainties.

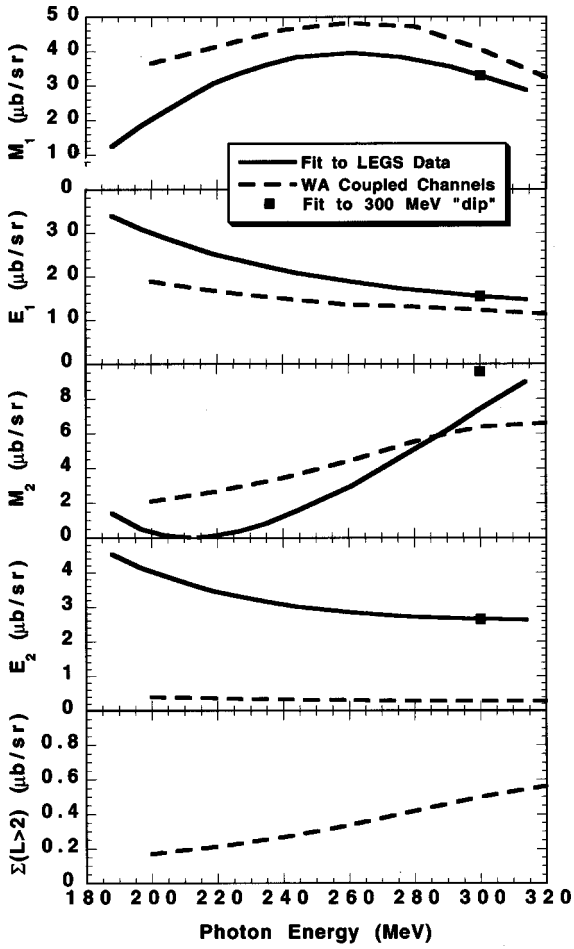

FIG. 1. The angle integrated total cross sections for each for the photon multipolarities included in the fit. The total integrated cross section is the sum of the four components. The solid line represents the energy-dependent fit, the dashed line indicates the WA coupled-channels calculation, and the filled square symbol shows the result of a fit to the coupled-channels predictions at 300 MeV.

The fact that no renormalization is required indicates that the expansion is not truncated at so low an angular momentum that compensations are required by adjusting the scale factor. (The results of the final fit along with uncertainties computed using the complete error matrix can be accessed from the LEGS web page [18].)

To go beyond a direct comparison with the data, we have selected the WA coupled-channels calculation [4] as representative of the modern, sophisticated theoretical treatments. The $M1$, $E1$, $M2$, and $E2$ contributions to the total cross sections from our multipole decomposition are compared with that of the WA calculations in Fig. 1. The total cross section is the sum of these four terms [Eq. (1a)]. As expected, the $M1$ dominates near the peak of the Δ ($\approx$260 MeV for the γD system). There is, however, no clear expression of the Δ peak in other multipoles. This indicates that the mixing that occurs when transforming from the γN to the γD systems does not produce a major redistribution of the Δ strength. Nevertheless, the WA calculation produces a larger $M1$ strength than does the fit throughout the energy range. The reduced $M1$ strength appears to be required by the data, independent of the precise details of the fit. A variety of different fits made to the data (for example, see fits

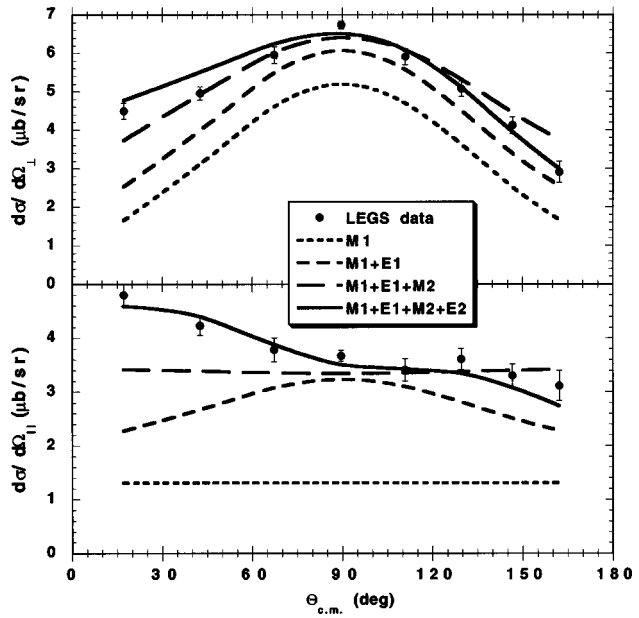

FIG. 2. The multipole decomposition of the parallel and perpendicular cross sections at 300 MeV. The cross sections are computed using the final fit described in Table I. The dotted line represents the $M1$ multipole strength. The medium dashed curve shows the sum of the $M1$ and $E1$, the long dashed line represents the sum of the $M1$, $E1$, and $M2$, and the solid line is the full fit to the data. The statistical uncertainties in the fits are smaller than the line thicknesses.

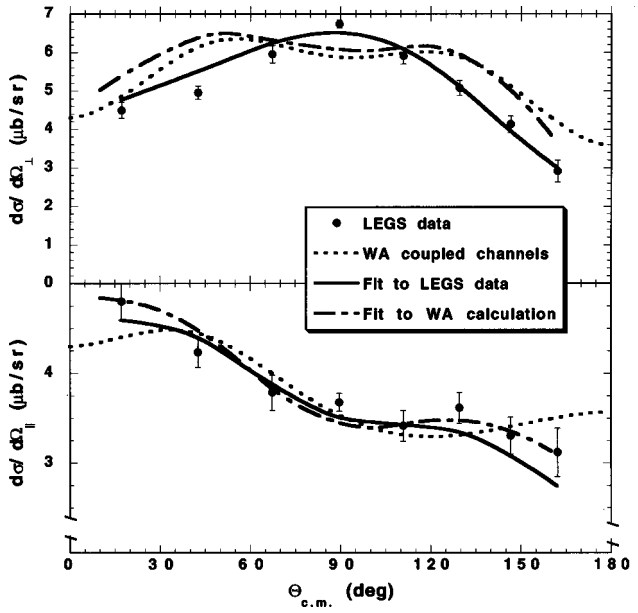

FIG. 3. The parallel and perpendicular cross sections at 300 MeV. The filled circles show the LEGS data and the solid lines represent the fit to this data. The dot-dashed lines represent the fit to a comparable number of points predicted by the full WA coupled-channels calculation. (The full WA calculation is shown as dotted lines.)

A–C in Table II below) all fall below the calculation. This may indicate a problem in coupled channels procedure.

The $E1$ multipole becomes increasingly important at the lower energies. The increase of $E1$ and decrease of $M1$ strength is more pronounced in the fit than in the WA calculation, although the energy dependences are similar.

The fitted $M2$ strength is similar in magnitude to that of WA. Although the energy dependences are somewhat different, both generally follow the same trend of increasing with photon energy.

The most striking difference occurs in the fitted $E2$ cross sections that are an order of magnitude larger than the WA calculation. As Donnachie has pointed out [19], the truncation of a multipole expansion can give rise to an ambiguity which can effectively shift strength from higher, omitted, terms down to lower angular momenta. To check whether this truncation ambiguity is responsible for the increased fitted $E2$ strength we have plotted in the lowest panel of Fig. 1 the sum of $E3$, $M3$, $E4$, and $M4$ cross sections from the WA calculation. Evidently, the increased $E2$ cross section is not caused by the absence of higher multipoles in the fit but rather results from a redistribution between dipole and quadrupole strength in our multipole analysis as compared to the WA calculation.

The multipole decomposition of the cross section at 300 MeV is shown in Fig. 2. The $\sigma_{\parallel}(90°)$ cross section is mostly $E1$. The $E1(^3F_3)$ and the $M2(^3F_3)$ contributions to $\sigma_{\parallel}$ have terms involving $\cos^2(\theta)$ which almost exactly cancel so that these, combined with the constant $M1$ term, lead to a nearly flat angular distribution. The forward-backward angle asymmetry is driven by the $E2$ multipole. Because the $E2$ strength is small and the angular dependence produced by the pure $E2$ terms contains only even powers of $\cos(\theta)$, this asymmetry comes from the $E2 \cdot E1$ interference which contributes $\cos(\theta)$ and $\cos^3(\theta)$ angular dependences and is amplified by the large $E1$ strength.

The fit reproduces the $\sigma_{\perp}$ cross sections with the $M1$ strength dominating, but the decomposition for $\sigma_{\perp}$ sheds no light on the possible sources of the predicted 90° dip. Because the fit and the calculation use different p-n phases and the energy dependences for the $M2$ and $E2$ contributions are different, a direct multipole by multipole comparison is not very illuminating. Rather, we have taken a simple, empirical approach to analyze the predicted 90° dip. Taking our fit to the LEGS data as an initial baseline, we have fit the predictions from the WA coupled-channels calculation. The difference between the fit to the data and the fit to the calculation then provides an indication of the source of the dip in the calculations. To avoid the complication of an energy dependence, we have focused on 300 MeV where the predicted dip is large (Fig. 3).

We replaced the 300 MeV LEGS data with predicted WA values selected at eight angles, assigned uncertainties typical of the LEGS data, and then repeated the fit at this one energy. A fit to these cross sections varying all eight multipoles included in the final fit could not reproduce the dip. To identify the multipoles which contribute to the dip, a series of additional fits was made, fixing the parameters to those of the final fit described in Table I, and then allowing one other multipole at a time to vary. All multipoles not already included in the final fit were sequentially varied in this procedure. Only with the addition of $M2(^3P_2)$ is the coupled-channel calculation reproduced. The fit to the LEGS data and this fit to the WA calculation at 300 MeV are shown along with the LEGS data in Fig. 3. The agreement between the

calculation and the fit for $\sigma_\perp$ is quite reasonable, *although* there are *some* differences at large and small angles for $\sigma_\parallel$. These extreme angles are sensitive to the interference of multipoles with natural and unnatural parity. Since WA include terms up to $L=4$ and our fit stops at $L=2$, differences from our fit are to be expected in this angular region.

The effect of this fit on the multipole strengths are indicated by the filled squares in Fig. 1. The addition of the $M2(^3P_2)$ multipole produces an increase in the $M2$ cross section and leaves the others unaffected. Since the effect is confined to the $M2$ cross section and only the $M2(^3F_3)$ and $M2(^3P_2)$ are nonzero, there are two terms to investigate: the $[M2(^3P_2)]^2$ and $M2(^3P_2)\cdot M2(^3F_3)$. By successively editing these terms from the multipole expansion and repeating the fit, we find that the $M2(^3P_2)\cdot M2(^3F_3)$ interference term is responsible for the 90° dip in $\sigma_\perp$.

We have also repeated the above procedure allowing all nine multipoles, the final eight plus one more, to vary each time (rather than fixing the final eight and varying only the added one). Now we find that many $M2$ multipoles either directly or through their interference with the $M2(^3F_3)$ can produce a dip at 90°, although the $M2(^3P_2)\cdot M2(^3F_3)$ is clearly preferred. In our fits, the dip is produced by a particular combination of constant, $\cos^2(\theta)$ and $\cos^4(\theta)$ terms. An overall negative $\cos^4(\theta)$ contribution creates the generally negative curvature, while positive constant and $\cos^2(\theta)$ terms produce an increase in the cross section near 50° and 130°. This combination can be produced in several ways but only by the $M2$ multipoles in our fit.

In the above analyses, multipole phases were fixed to the p-n elastic scattering values. The phases used in the WA calculation have been renormalized by the coupling with the $N\Delta$ interaction and are considerably different. To test the model dependence of conclusions regarding the source of the asymmetry in $\sigma_\parallel$ and the predicted dip in $\sigma_\perp$ to the multipole phases we have made another series of fits at 300 MeV, both to the LEGS data and to the WA calculation, using the coupled-channel phases of WA. The angle integrated cross sections from these fits, along with those of the final fit described in Table I and the full WA calculation, are given in Table II. The fit labeled A starts with the eight multipoles included in the final fit of Table I and refits the LEGS data at 300 MeV with the WA phases. Fit D is a repeat of fit A with the LEGS data replaced by predictions from the WA calculation. Solution A is very similar to the final fit, except for an exchange between $M2$ and $E2$ strengths. Comparing solution D to the full WA calculation, both $M2$ and $E2$ components have increased at the expense of the $M1$ strength.

To test the sensitivity of the fitting procedure to the initial starting point of the chi-squared minimization we have repeated A and D, but starting from the WA values of the eight multipoles rather than the final fit values. The results are shown in columns B and E in Table II. Fits C and F again vary only the eight multipoles included in the final fit, but start with all 22 $L\leqslant 2$ multipoles set to the WA values.

The $M1$ strength is relatively stable in the fits to the LEGS data (sets A, B, and C), but the other multipoles vary quite a bit. In fact, for fits B and C the $E2$ multipole is larger than either the $E1$ or $M2$. In spite of the fact that all of these fits reproduce the LEGS data very well, there are significant redistributions of the multipole strength when compared to the final fit. The range of solutions which fit the data reflects the ambiguity inherent to the limited number of observables available. In these fits, the $M2$ strength is small and there is an exchange of strength between the $E1$ and $E2$ multipoles: smaller $E1$ contributions are accompanied by larger $E2$ terms. A detailed decomposition of each of these fits shows that the forward-backward asymmetry in $\sigma_\parallel$ is still produced by the $E2\cdot E1$ interference. Thus, regardless of the nature of the fit, $\sigma_\parallel$ is dominated by the electric multipoles and the $E2\cdot E1$ interference term is responsible for the asymmetry in the observed angular distribution.

TABLE II. The angle integrated cross sections at 300 MeV for each of the photon multipoles included in the fit. The total cross section is the sum of the terms as indicated by Eq. (1a). The fit labeled final is described in Table I—there the multipole phases were fixed at the corresponding elastic p-n values. For all of the other columns of this table multipole phases were fixed at the coupled-channels values from WA [4]. The column labeled full WA calculation includes all multipoles with $L\leqslant 4$. Solutions A and D start the χ^2 minimization from the final fit values, while B and E start at the WA values for the eight multipoles of the final fit. Solutions C and F start with all $L\leqslant 2$ multipoles fixed at the WA values but vary only the eight of the final fit. All cross sections are in μb.

		Fit to LEGS data				Fit to WA dip		
Multipole	Final	A	B	C	Full WA	D	E	F
$M1$	32.9	35.1	37.9	34.8	40.5	24.5	8.3	0.1
$E1$	15.4	13.0	1.1	5.2	12.3	12.9	20.2	23.0
$M2$	7.4	1.1	1.1	2.3	6.4	17.0	32.7	28.0
$E2$	2.6	8.9	17.1	15.9	0.3	4.5	5.9	7.7
$L>2$	0	0	0	0	0.5	0	0	0
Total	58.3	58.1	57.1	58.2	59.9	58.9	67.1	58.8

Fits D and E, which include only one $M2$ multipole, the $M2(^3F_3)$, do not reproduce the predicted dip at 90° in $\sigma_\perp$. However, the nonphysical fit F (with negligible $M1$ strength) includes nonzero values for all the $M2$ multipoles and does fit the dip. A more detailed examination of this fit shows that once again, the $M2(^3P_2)$ is required to produce the dip. If, as before, other $M2$ multipoles are also allowed to vary along with the eight in fit F, then again several $M2$ multipoles can make a 90° dip in $\sigma_\perp$.

The WA coupled-channel calculation includes multipoles up to $L\leqslant 4$. Their $M2(^3P_2)$ strength is smaller than in our fits, and a significant fraction of the dip in the $\sigma_\perp(90°)$ prediction comes from $M1(^1D_2)\cdot M3(^1G_4)$ interference [4]. Once again, both the magnitude of the $\sigma_\perp$ cross section and the shape of its angular distribution are dominated by the magnetic multipoles.

Meson exchange currents (MEC's) are well known to generate sizable effects in $D(\gamma,p)n$ in the energy range of this study [5]. It is interesting to recall that current conservation allows the evaluation of the dominant part of electric MEC transitions directly from the charge density, without requiring explicit knowledge of the nuclear current. This is just Siegert's theorem and has been used in most of the coupled-channels calculations. However, evaluation of the

magnetic MEC transitions requires the nuclear current. In light of this, it is very tempting to speculate that the agreement in Fig. 3 between the WA calculation and $\sigma_{\parallel}$, which is dominated by electric transitions, is due to the essentially perfect treatment of the electric MEC components that is guaranteed by Siegert's theorem. Conversely, the failure of the WA calculation to reproduce the $\sigma_{\perp}$ distribution suggests problems with the hadronic current that is needed to evaluate the magnetic MEC contributions, since it is the magnetic multipoles that dominate $\sigma_{\perp}$.

To summarize, we have carried out the first multipole analysis of the photodisintegration of deuterium in the Δ resonance region, using recent data taken with linearly polarized photons. In an expansion that includes electric and magnetic dipole and quadrupole radiation, the data can be fit with 11 parameters specifying the energy dependence of 8 multipoles. Solutions of equivalent quality can be obtained with a larger number of parameters and we have examined the multipole decompositions of a wide variety. In all cases, the parallel cross section is dominated by electric multipoles and the forward-backward asymmetry that characterizes the angular dependence of the $\sigma_{\parallel}$ data is produced by $E2 \cdot E1$ interference. In contrast, the perpendicular cross sections are dominated by magnetic multipoles, and a spurious 90° dip in the $\sigma_{\perp}$ predictions that characterize all recent coupled-channel calculations can be reproduced by changing the $M2$ strength distribution in our fit.

While the WA calculations are in good agreement with the electric-multipole-dominated $\sigma_{\parallel}$ data, they predict a shape for the magnetic-dominated $\sigma_{\perp}$ distribution that is clearly inconsistent with the measurements. We speculate that this rather unusual situation could be caused by an incomplete treatment of MEC's which affects primarily the magnetic transitions where the hadronic currents are important. It is clearly desirable to further reduce the ambiguities in the multipole decomposition. For this, other polarization observables are required, and many are expected to be sensitive to nuclear potentials and currents [20]. Although there is a limited amount of nucleon polarization data [21,22], the few points currently available in the region of the Δ resonance [21] have nearly 100% errors and do not provide a useful constraint. However, beam-target double-polarization experiments are in preparation at the LEGS and Mainz tagged photon facilities and these are likely to change this situation dramatically.

We would like to thank Dr. H. Arenhövel and Dr. P. Wilhelm for many stimulating interactions. This work was supported by the U.S. Department of Energy under Contract No. DE-AC02-76CH00016, and by the National Science Foundation.

[1] W. Leidemann and H. Arenhövel, Nucl. Phys. **A465**, 573 (1987).
[2] M. T. Peña, H. Garcilazo, U. Oelfke, and P. U. Sauer, Phys. Rev. C **45**, 1487 (1992).
[3] G. S. Blanpied *et al.*, LEGS Collaboration, Phys. Rev. Lett. **67**, 1206 (1991); W. K. Mize, Ph.D. thesis, University of South Carolina, 1992, Brookhaven National Lab Report No. LEGS-92T1 1992.
[4] P. Wilhelm and H. Arenhövel, Phys. Lett. B **318**, 410 (1993); (private communication).
[5] H. Tanabe and K. Ohta, Phys. Rev. C **40**, 1905 (1989).
[6] T.-S. H. Lee, *5th Workshop on Perspectives in Nuclear Physics at Intermediate Energies*, ICTP Trieste, Italy, May, 1991 (World Scientific, Singapore, 1992).
[7] G. S. Blanpied *et al.*, LEGS Collaboration, Phys. Rev. C **52**, R455 (1995).
[8] W. Leidemann and H. Arenhövel, Can. J. Phys. **62**, 1036 (1984).
[9] J.-M. Laget, Can. J. Phys. **62**, 1046 (1984).
[10] H. Arenhövel and M. Sanzone, Few-Body Syst., Suppl. **3**, 1 (1991).
[11] LEGS Data Release L1-3.0, March, 1994, from URL http://www.legs.bnl.gov/.
[12] H. Weller, J. Lanenbrunner, R. M. Chasteler, E. L. Tomusiak, J. Asai, R. G. Seyler, and D. R. Lehman, At. Data Nucl. Data Tables **50**, 29 (1992).
[13] K. M. Watson, Phys. Rev. **95**, 228 (1954).
[14] The Scattering Analysis Interactive Dial-in (SAID) program, available by TELNET to VTINTE.PHYS.VT.EDU {physics, quantum}.
[15] MINUIT 95.03, CERN Library D506, CERN, 1995.
[16] Philip R. Bevington and D. Keith Robinson, *Data Reduction and Error Analysis for the Physical Sciences*, 2nd ed. (McGraw-Hill, New York, 1969).
[17] G. D'Agostini, Nucl. Instrum. Methods Phys. Res. A **346**, 306 (1994).
[18] The program generating cross sections and uncertainties from the fit is accessible at URL http://www.legs.bnl.gov/.
[19] A. Donnachie, Rep. Prog. Phys. **36**, 695 (1973).
[20] K.-M. Schmitt and H. Arenhövel, Few-Body Syst., Suppl. **4**, 1 (1991).
[21] F. F. Liu, D. Lundquist, and B. Wilk, Phys. Rev. **165**, 1478 (1968).
[22] M. Hugi *et al.*, Nucl. Phys. **A472**, 701 (1987).